

## FTIR SPECTRAL CHANGES IN *Candida albicans* BIOFILM FOLLOWING EXPOSURE TO ANTIFUNGALS

ALYA NUR ATHIRAH KAMARUZZAMAN<sup>1</sup>, TENGGU ELIDA TENGGU ZAINAL MULOK<sup>1</sup>, NURUL HIDAYAH MOHAMAD NOR<sup>2</sup> and MOHD FAKHARUL ZAMAN RAJA YAHYA<sup>1\*</sup>

<sup>1</sup>Faculty of Applied Sciences, Universiti Teknologi MARA, 40450 Shah Alam, Selangor, Malaysia

<sup>2</sup>Low Dimensional Materials Research Centre, Department of Physics, Faculty of Science, University of Malaya, 50603 Kuala Lumpur, Malaysia

\*E-mail: fakhirulzaman@uitm.edu.my

Accepted 3 October 2022, Published online 31 October 2022

### ABSTRACT

*Candida albicans* is a microbial fungus that exists as a commensal member of the human microbiome and an opportunistic pathogen. Biofilm formation by this fungal pathogen occurs mostly in the mucosa or endothelium associated with candidiasis and colonizes medical devices. The present work was performed to determine the efficacy of the antifungal creams on the viability and biochemical composition of *C. albicans* biofilm. Four commercial antifungal creams were used herein namely econazole nitrate, miconazole nitrate, ketoconazole and tolnaftate. Resazurin assay and Fourier transform infrared (FTIR) spectroscopy were performed to determine the viability and biochemical composition of *C. albicans* biofilm, respectively. Results demonstrated that the antifungal creams inhibited *C. albicans* biofilm. The highest percent inhibition shown by econazole nitrate, miconazole nitrate, ketoconazole, and tolnaftate were 16.5%, 17.1%, 15.8%, and 6.9%, respectively. Econazole nitrate with the lowest IC<sub>50</sub> value of 43.42 µg/mL caused changes in the FTIR spectral peak shape at 1377 cm<sup>-1</sup> and 1736 cm<sup>-1</sup>. On the other hand, miconazole nitrate with the second lowest IC<sub>50</sub> value of 118.26 µg/mL caused spectral peak shifting from 1237 cm<sup>-1</sup> to 1228 cm<sup>-1</sup>. In conclusion, the inhibition of *C. albicans* biofilm may be mediated by the changes in protein, lipid, and nucleic acid compositions.

**Key words:** *Candida*, fungal pathogen, biofilm formation, antibiofilm, FTIR spectroscopy

### INTRODUCTION

*Candida* species cause a wide spectrum of fungal infections (Hani *et al.*, 2015). There are about 400,000 cases of fungal diseases with the rate of mortality up to 40% due to *Candida* species. *Candida* species can be found in the oral cavity, gastrointestinal tract, vagina, and mucosal skin. This genus is composed of different *Candida* species that are known to cause infections almost 90% due to *Candida albicans*, *Candida glabrata*, *Candida parasilopsis*, and *Candida krusei*. It may lead to non-fatal illnesses and also persistent infections in humans. *C. albicans* remains the major clinical problem causing infections among all *Candida* species (Silva *et al.*, 2017; Pebotuwa *et al.*, 2020). Common antifungals used to control *C. albicans* infections include econazole nitrate, miconazole nitrate, ketoconazole and tolnaftate. According to Marak and Dhanashree (2018), fungal diseases and infections are mainly caused by *C. albicans* biofilm formation, where the biofilm is an assembly of microorganisms that are entrenched in an extracellular matrix on biotic and abiotic surfaces (Hasan *et al.*,

2009; Yaacob *et al.*, 2021). Understanding structure, proteins, biological pathways, and other biofilm components are the key to biofilm control strategy (Yahya *et al.*, 2014; Othman & Yahya, 2019).

The biofilm formed by *C. albicans* involves several stages of growth which are the formation of round budding cells, oval pseudohyphal cells, and cylindrical hyphal cells that are surrounded by an extracellular matrix (ECM). Overgrowth of *C. albicans* mainly due to biofilm growth develops candidiasis that occurs inside of the mouth, gut, throat, vagina as well as skin. A mature biofilm forms in the duration of 24 h and can be observed as a cloudy formation of the top solid surface and under the microscope (Gulati & Nobile, 2016). The maturation of *C. albicans* biofilm displays its characteristics such as in the form of complex three-dimensional (3-D) structure and extensive spatial heterogeneity which is encased in exopolymeric material (Ramage *et al.*, 2006). This fungal species also tend to form polyspecies biofilm with bacteria (Isa *et al.*, 2022).

Fourier Transform Infrared (FTIR) spectroscopy is a non-destructive technique commonly used to observe the changes in the biochemical composition of fungal cells (Quilès *et al.*, 2017). It is useful for

\* To whom correspondence should be addressed

the analysis of molecules and cellular components in a different range of sizes such as carbohydrates, lipids, proteins, and nucleic acids (Berthomieu & Hienerwadel, 2009; Zhang *et al.*, 2017; Aging & Munajad, 2018). In the last few decades, the application of FTIR spectroscopy in antimicrobial studies has received great attention. Until now, the information on FTIR spectral changes of *C. albicans* biofilm following exposure to antifungals is still limited.

## MATERIALS AND METHODS

### Preparation of test microorganism

*Candida albicans* ATCC MYA-2876 was obtained from the Microbiology Culture Collection, Faculty of Applied Sciences, UiTM Shah Alam, Selangor, Malaysia. *C. albicans* was transferred into a 50 mL conical flask containing 26 mL of potato dextrose broth (Friendemann Schmidt, Australia). The fungal culture was incubated at 37 °C for 48 h without agitation. After incubation, the fungal culture turbidity was standardized by dilution and using a spectrophotometer to achieve a turbidity reading of 0.6-0.8 at 600 nm for biofilm assay. Gram staining was carried out to assess colony morphology and colony purity.

### Preparation of antifungal creams

Table 1 shows a list of antifungal creams used in the present study. Antifungal cream of 5000 µg/mL was prepared and serially diluted with distilled water into 2500 µg/mL, 1250 µg/mL, 625 µg/mL, 312.5 µg/mL and 156.25 µg/mL solutions (Bojsen *et al.*, 2014). The dilutions were done by stirring the solutions at 60°C and allowing the mixture to be fully dissolved (Alsterholm *et al.*, 2010).

### Biofilm formation assay in 96-well microtiter plate for resazurin assay

One hundred fifty µL of *C. albicans* culture and 50 µL of the topical antifungal cream solutions were loaded into 96-well microtiter plates. The wells containing 150 µL of fungal culture and 50 µL of PDB were used as negative controls. The wells containing 150 µL of fungal culture and 50 µL of intellectual property (IP)-protected antibiofilm cocktail were

used as positive controls. The microtiter plates were incubated overnight at 37 °C.

### Resazurin assay

For the resazurin assay, the broth in the microtiter plates from the previous step was discarded after 24 h of incubation, and the microtiter plate was then washed three times using sterile distilled water to remove the non-adherent cells. A volume of 150 µL of phosphate buffer saline (PBS) with 50 µL of resazurin solution was then added to the microtiter plate wells. Any color change was observed after 24 h of incubation (Coban *et al.*, 2012). The absorbance of viable cells was measured at the 570 nm wavelength by using a microplate reader. The percentage of inhibition for biofilm viability was calculated using the formula as follows:

Equation 1:

$$\text{Percentage of inhibition} = \frac{\text{control wells} - \text{experimental wells}}{\text{control wells}} \times 100$$

The half-maximum inhibitory concentration (IC<sub>50</sub>) values for the inhibition study of *C. albicans* biofilm were calculated using Quest Graph™ IC<sub>50</sub> Calculator.

### Biofilm formation assay in 6-well microtiter plate for FTIR spectroscopy

Three mL of *C. albicans* culture and one mL of topical antifungal cream solutions were loaded into 6-well microtiter plates. The wells containing three mL of fungal culture and one mL of potato dextrose broth were used as negative controls. The wells containing three mL of fungal culture and one mL of intellectual property (IP)-protected antibiofilm cocktail were used as positive controls. The microtiter plate was incubated overnight at 37 °C.

### FTIR spectroscopy

Determination of the biochemical composition of *C. albicans* biofilm was performed as previously reported (Yahya *et al.*, 2018). Following incubation at 37 °C for 24 h, the contents in all wells of the microtiter plates were discarded. The wells were then rinsed twice using sterile distilled water. The biofilm fractions were then scraped from the walls of the wells using a sterile spatula in the presence of

**Table 1.** The active ingredients in each type of topical antifungal creams

Type of antifungal creams	Active ingredient	Fungicidal/Fungistatic
Antifungal cream A	Econazole nitrate	Fungistatic
Antifungal cream B	Miconazole nitrate	Fungistatic
Antifungal cream C	Ketoconazole	Fungistatic
Antifungal cream D	Tolnaftate	Fungicidal and fungistatic

0.9% NaCl, 1 mM PMSF (Sigma, USA), and 10  $\mu$ L of 1% SDS (Sigma, USA). Then, the suspensions in the microtiter plate wells were transferred into sterile 1.5 mL microcentrifuge tubes and vortexed for three min. The tubes were then centrifuged at 4,000  $g$  for 15 min at 4  $^{\circ}$ C. The resulting cell pellets were dried for two h at 60  $^{\circ}$ C. The dried pellets were then scraped from the 1.5 mL microcentrifuge tubes using a sterile stainless-steel ear pick and were positioned in direct contact with the diamond crystal in the Perkin Elmer Spectrum One FTIR spectrometer (System 2000, Perkin Elmer, Wellesly, MD, USA) and scanned for infrared spectral analysis. The biofilm analysis was performed in the wavenumber range between 3000  $\text{cm}^{-1}$  and 600  $\text{cm}^{-1}$  at a resolution of four  $\text{cm}^{-1}$ . Data collection, visualization, and processing were performed using the Spectrum 10 Spectroscopy software (Perkin Elmer, Inc.). A total of eight infrared (IR) spectra were acquired from each of the samples to generate a spectrum of the biochemical composition of *C. albicans* biofilm treated with antifungal creams.

## RESULTS AND DISCUSSION

### Inhibition of *C. albicans* biofilm

Figure 1 shows the viability of *C. albicans* biofilm in the presence of antifungal creams. Treatment with the tested antifungal creams was found to inhibit the

viability of *C. albicans* biofilm. The highest percent inhibition shown by econazole nitrate, miconazole nitrate, ketoconazole, and tolnaftate-based antifungal creams were 16.5%, 17.1%, 15.8%, and 6.9%, respectively. Two test concentrations of tolnaftate-based antifungal cream (156.25  $\mu\text{g}/\text{mL}$  & 312.5  $\mu\text{g}/\text{mL}$ ) did not show any inhibitory action against *C. albicans* biofilm. On the other hand, the  $\text{IC}_{50}$  values shown by econazole nitrate, miconazole nitrate, ketoconazole, and tolnaftate-based antifungal creams were 43.42  $\mu\text{g}/\text{mL}$ , 118.26  $\mu\text{g}/\text{mL}$ , 99.93  $\mu\text{g}/\text{mL}$  and 10240  $\mu\text{g}/\text{mL}$  respectively.

### FTIR assignment of functional groups

Table 2 shows the FTIR assignments of functional groups detected in *C. albicans* biofilm. A total of 32 spectral peaks in the range between 3000  $\text{cm}^{-1}$  and 600  $\text{cm}^{-1}$  were classified into four categories namely lipids, proteins, nucleic acids, and polysaccharides.

### Econazole nitrate-based antifungal cream

Figure 2 shows the FTIR spectra for *C. albicans* biofilm in the presence of antifungal cream A. Treatment with the econazole nitrate-based antifungal cream caused changes in the spectral peak shape at 1377  $\text{cm}^{-1}$  (all test concentrations), and 1736  $\text{cm}^{-1}$  (5000  $\mu\text{g}/\text{mL}$ ).

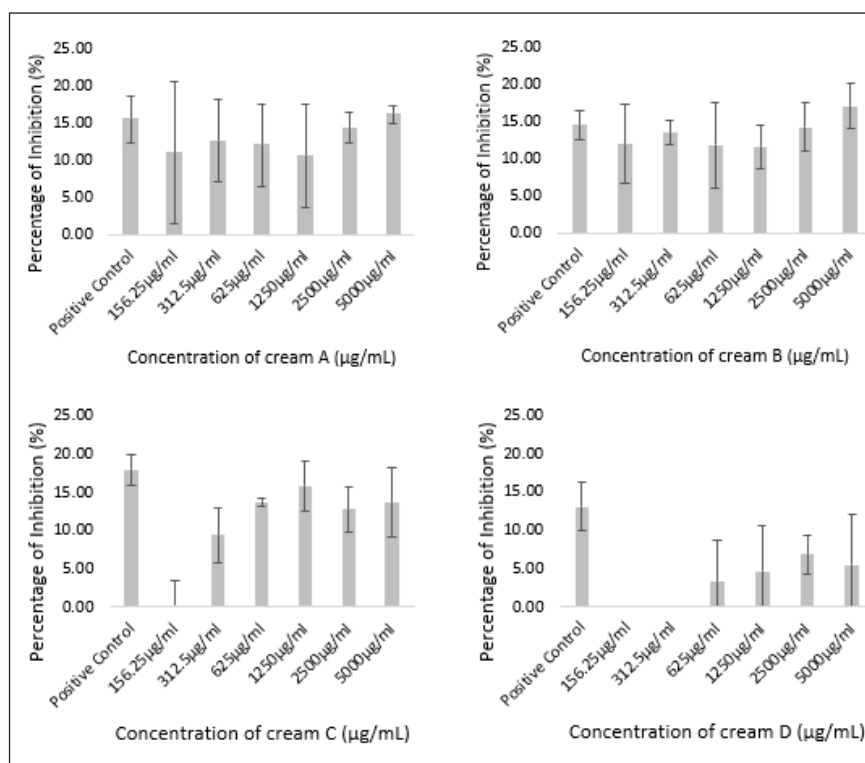


**Fig. 1.** Effects of antifungal creams on the viability of *C. albicans* biofilm. Cream A: econazole nitrate-based antifungal cream; Cream B: miconazole nitrate-based antifungal cream; Cream C: ketoconazole-based antifungal cream; Cream D: tolnaftate-based antifungal cream. Each bar represents mean  $\pm$  standard deviation,  $n=3$ . Positive control: fungal inoculum mixed with IP-protected antibiofilm cocktail. Negative control: fungal inoculum mixed with fresh broth.

**Table 2.** FTIR assignments of *C. albicans* biofilm components

Wavenumber (cm <sup>-1</sup> )	IR assignment	Classification
2925, 2924, 2922, 2919	CH <sub>2</sub> asymmetric stretching	Lipid
2856, 2854, 2853, 2851	CH <sub>2</sub> symmetric stretching	Lipid
1740, 1736, 1735	C=O stretching of lipid ester	Lipid
1631, 1628	(C=O stretching) Amide I	Protein
1540, 1534, 1533, 1532	(CONH bending) Amide II	Protein
1378, 1377, 1373	(C-N stretching vibration/N-H bending vibration) Amide III	Protein
1237, 1235, 1219, 1218	PO <sub>2</sub> <sup>-</sup> asymmetric stretching	Nucleic acid
1032, 1027, 1024, 1018	C-O stretching	Polysaccharide
810, 809, 808, 807	α-mannans	Polysaccharide

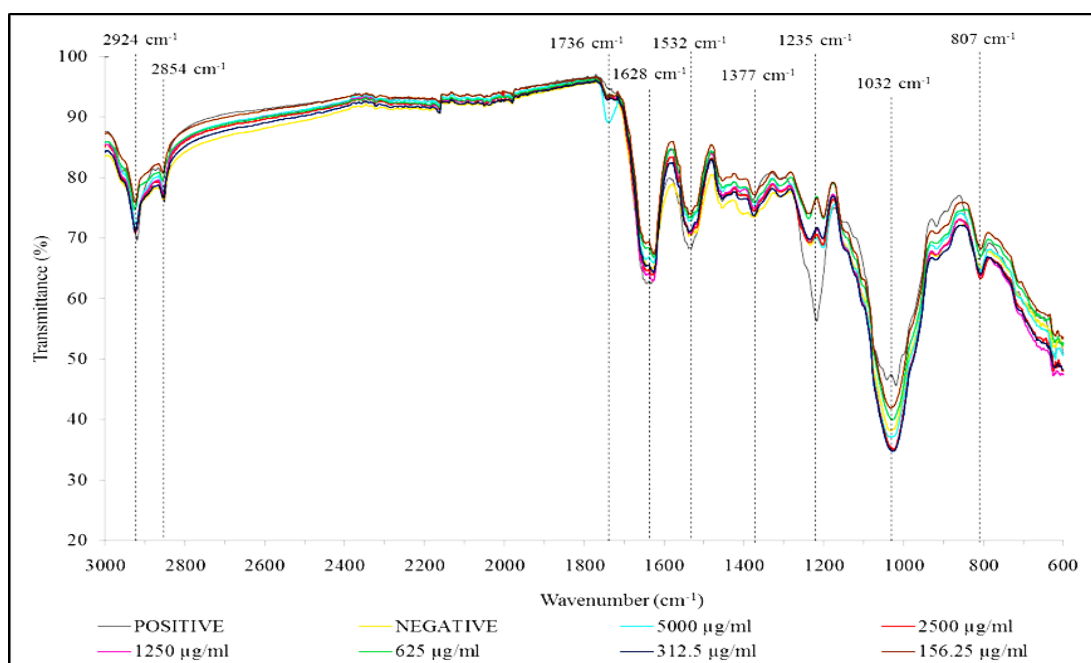


**Fig. 2.** FTIR spectra of *C. albicans* biofilm exposed to the econazole nitrate-based antifungal cream. The spectra were measured in the range between 3000 cm<sup>-1</sup> and 600 cm<sup>-1</sup>. Positive control: fungal inoculum mixed with the IP-protected antibiofilm cocktail. Negative control: fungal inoculum mixed with fresh broth.

#### Miconazole nitrate-based antifungal cream

Figure 3 shows the FTIR spectra for *C. albicans* biofilm in the presence of cream B. Treatment with 156.25 µg/mL of the miconazole nitrate-based antifungal cream caused a spectral peak shifting from 1237 cm<sup>-1</sup> to 1228 cm<sup>-1</sup> while 5000 µg/mL caused the disappearance of a spectral peak at 1237 cm<sup>-1</sup>.

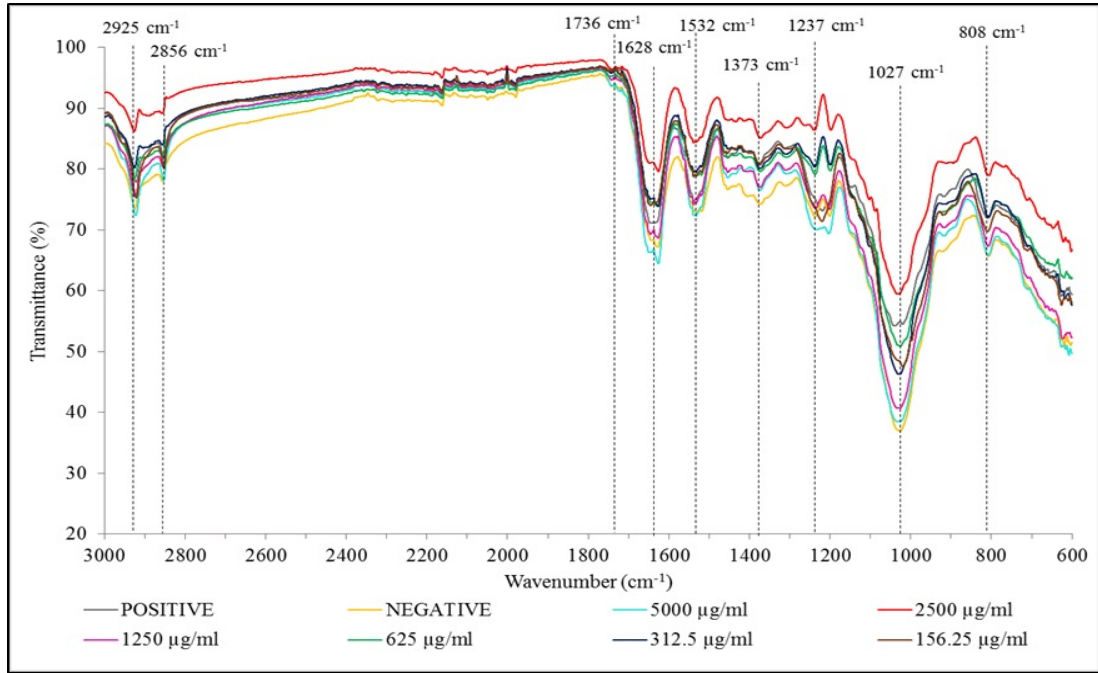
#### Ketoconazole nitrate-based antifungal cream

Figure 4 shows the FTIR spectra for *C. albicans* biofilm in the presence of cream C. All test concentrations of the ketoconazole nitrate-based antifungal cream were found to cause a spectral peak sharpening at 1378 cm<sup>-1</sup>.

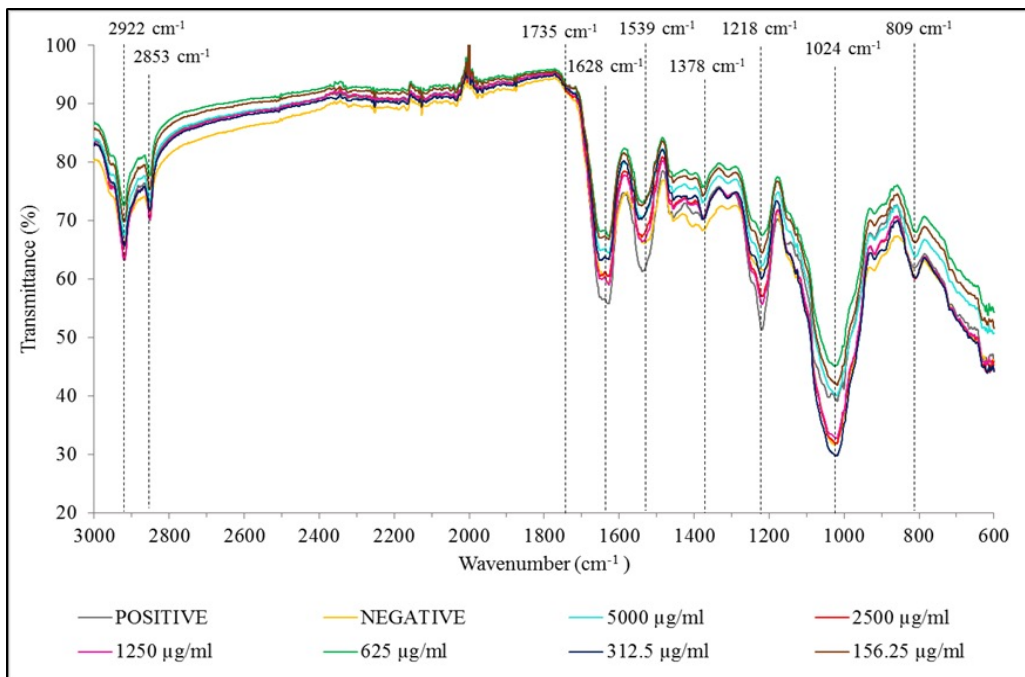
#### Tolnaftate-based antifungal cream

Figure 5 shows the FTIR spectra for *C. albicans* biofilm in the presence of cream D. Treatment with 2500 µg/mL and 5000 µg/mL of the tolinaftate-based antifungal cream increased the spectral peak size at 1019 cm<sup>-1</sup>.

Econazole nitrate is an imidazole antifungal agent with fungistatic properties against a wide range of yeasts and fungi. The molecular mechanism of econazole nitrate involves the inhibition of ergosterol biosynthesis that could damage the fungal cell wall membrane. Furthermore, inhibition of ergosterol biosynthesis also increases the membrane permeability which causes loss of cellular contents. The present



**Fig. 3.** FTIR spectra of *C. albicans* biofilm exposed to the miconazole nitrate-based antifungal cream. The spectra were measured in the range between 3000  $\text{cm}^{-1}$  and 600  $\text{cm}^{-1}$ . Positive control: fungal inoculum mixed with the IP-protected antibiofilm cocktail. Negative control: fungal inoculum mixed with fresh broth.



**Fig. 4.** FTIR spectra of *C. albicans* biofilm exposed to the ketoconazole nitrate-based antifungal cream. The spectra were measured in the range between 3000  $\text{cm}^{-1}$  and 600  $\text{cm}^{-1}$ . Positive control: fungal inoculum mixed with the IP-protected antibiofilm cocktail. Negative control: fungal inoculum mixed with fresh broth.

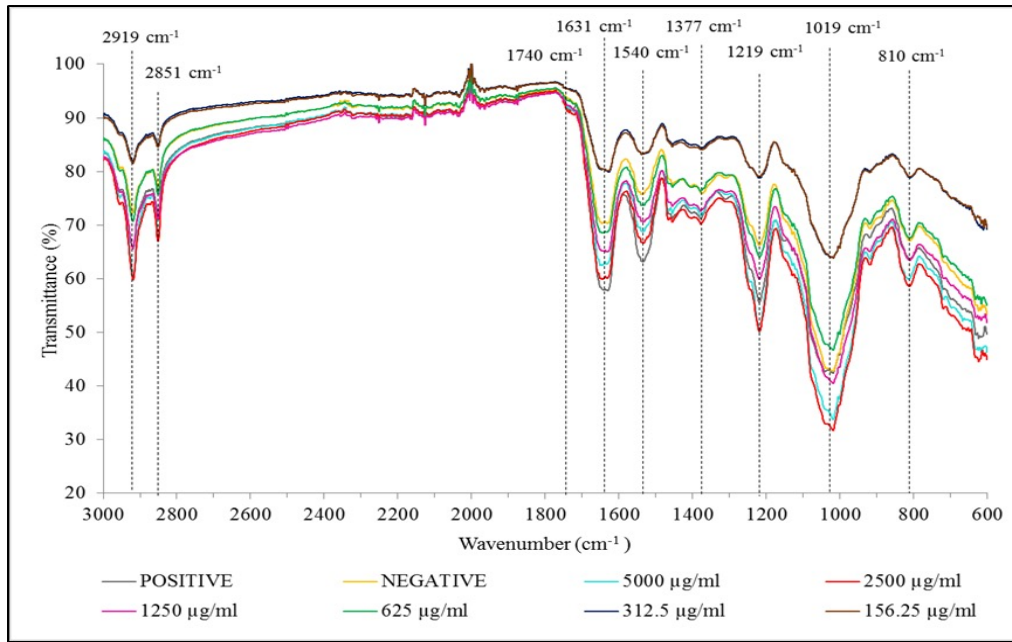


**Fig. 5.** FTIR spectra of *C. albicans* biofilm exposed to the tolnaftate-based antifungal cream. The spectra were measured in the range between 3000  $\text{cm}^{-1}$  and 600  $\text{cm}^{-1}$ . Positive control: fungal inoculum mixed with the IP-protected antibiofilm cocktail. Negative control: fungal inoculum mixed with fresh broth.

study showed the efficacy of econazole nitrate-based antifungal cream against *C. albicans* biofilm. The study on the inhibitory activity of econazole against fungal biofilm is still limited. However, econazole had shown inhibitory activity against the free-floating form of *C. albicans* and also inhibits *Streptococcus mutans* biofilm formation (Qiu *et al.*, 2017).

Miconazole nitrate is an antifungal medication that belongs to the imidazole group which is commonly used to treat fungal or yeast infections of the skin and vagina. It is known to inhibit the fungal enzyme  $14\alpha$ -sterol demethylase which is a component of fungal cell membranes. Inhibition of the  $14\alpha$ -sterol demethylase leads to decreased ergosterol production. In the present study, the miconazole nitrate-based antifungal cream was found to effectively inhibit the viability of *C. albicans* biofilm. This finding corroborates Gebremedhin *et al.* (2014) who demonstrated high antifungal activity of miconazole against *C. albicans* biofilm.

Ketoconazole is an antifungal imidazole drug that is administered in both oral and topical forms. Ketoconazole is known to inhibit the enzyme cytochrome P-450  $14\alpha$ -demethylase and blocks the formation of ergosterol, the key component of the fungal cell membrane. In the present study, the ketoconazole-based antifungal cream effectively inhibited the viability of *C. albicans* biofilm. This result is in agreement with Abd *et al.* (2014) demonstrating that ketoconazole was able to reduce biofilm formation by *C. albicans* in the range between 22% and 80.7%.

Tolnaftate is a synthetic thiocarbamate used as an

antifungal agent. The antifungal activity of tolnaftate has been elucidated since 1986 (Ryder *et al.*, 1986), though its fungicidal action is not completely understood. However, it may inhibit squalene epoxidase, an important enzyme in the ergosterol biosynthetic pathway. A previous study by Waghule *et al.* (2020) reported that tolnaftate could inhibit *C. albicans* strains through the inhibition of squalene epoxidase. In the present study, the tolnaftate-based antifungal cream managed to slightly inhibit the *C. albicans* biofilm. To our knowledge, the present study provides the first evidence of the antibiofilm activity of tolnaftate against *C. albicans*.

Lipids have been categorized as an important component of the extracellular matrix which functions to protect the biofilm. In the present study, the spectral peaks at 2925  $\text{cm}^{-1}$ , 2924  $\text{cm}^{-1}$ , 2922  $\text{cm}^{-1}$  and 2919  $\text{cm}^{-1}$  were identified in the FTIR spectra of *C. albicans* biofilm and were assigned to the  $\text{CH}_2$  asymmetric stretching mode of fatty acids. Furthermore, the spectral peaks at 2856  $\text{cm}^{-1}$ , 2854  $\text{cm}^{-1}$ , 2853  $\text{cm}^{-1}$  and 2851  $\text{cm}^{-1}$  were assigned to the  $\text{CH}_2$  symmetric stretching mode of fatty acids. These results are in line with Adt *et al.* (2006) showing that the FTIR spectral peaks at 2924  $\text{cm}^{-1}$  and 2851  $\text{cm}^{-1}$  were associated with the lipid macromolecule group in *C. albicans*. Moreover, the spectral peak at 1740  $\text{cm}^{-1}$ , 1736  $\text{cm}^{-1}$  and 1735  $\text{cm}^{-1}$  were assigned to the C=O stretching vibrations of lipid ester carbonyl. Multiple works have shown that these FTIR spectral peaks represent lipid biomolecules in *C. glabrata* and *C. albicans* biofilm (Bhat, 2013; Shi *et al.*, 2018; Pebotuwa *et al.*, 2020).

Proteins are crucial in maintaining structural

integrity, facilitating adherence, and host colonization in the development of biofilm. In the present study, the spectral peaks at 1631  $\text{cm}^{-1}$  and 1628  $\text{cm}^{-1}$  were identified in *C. albicans* biofilm and were assigned to the C=O stretching mode of amide I. This result is supported by Fiołka *et al.* (2020) showing that the amide I spectral peak of *C. albicans* was in the range of 1650  $\text{cm}^{-1}$  to 1515  $\text{cm}^{-1}$ . The FTIR spectral peak at 1540  $\text{cm}^{-1}$ , 1534  $\text{cm}^{-1}$ , 1533  $\text{cm}^{-1}$  and 1532  $\text{cm}^{-1}$  were assigned to the CONH bending of amide II. This result is in agreement with Shapaval *et al.* (2019) which reported the spectral peak of yeasts in the range between 1580  $\text{cm}^{-1}$  and 1520  $\text{cm}^{-1}$  representing amide II. Furthermore, the FTIR spectral peak at 1378  $\text{cm}^{-1}$ , 1377  $\text{cm}^{-1}$  and 1373  $\text{cm}^{-1}$  were assigned to the N-H bending and C-N stretching vibration of proteins (amide III). This result is supported by Natalello *et al.* (2005) and Naseer *et al.* (2020) showing the spectral peak for amide III in the range between 1400  $\text{cm}^{-1}$  and 1300  $\text{cm}^{-1}$ .

Nucleic acid is an important component of biofilm which carry several essential functions including initial adhesion, cell aggregation, and biofilm cohesion. In the present study, the spectral peaks at 1237  $\text{cm}^{-1}$ , 1235  $\text{cm}^{-1}$ , 1219  $\text{cm}^{-1}$  and 1218  $\text{cm}^{-1}$  were identified in the FTIR spectra of *C. albicans* biofilm and were assigned to  $\text{PO}_2^-$  asymmetric stretching of nucleic acid group. This result is in agreement with Sockalingum *et al.* (2002) demonstrating the spectral peak for  $\text{PO}_2^-$  asymmetric stretching (1180  $\text{cm}^{-1}$  & 1300  $\text{cm}^{-1}$ ) found in the FTIR spectra of *C. albicans* isolates.

Polysaccharides play a role in providing structure to biofilm and providing protection from a wide range of stresses including desiccation and predators (phagocytic cells). In the present study, the spectral peaks at 1032  $\text{cm}^{-1}$ , 1027  $\text{cm}^{-1}$ , 1024  $\text{cm}^{-1}$  and 1018  $\text{cm}^{-1}$  were identified in the FTIR spectra of *C. albicans* biofilm and were assigned to the C-O stretching of polysaccharides. On the other hand, the identified spectral peak at 810  $\text{cm}^{-1}$ , 809  $\text{cm}^{-1}$ , 808  $\text{cm}^{-1}$  and 807  $\text{cm}^{-1}$  were assigned to the  $\alpha$ -mannans. These results are by Pebotuwa *et al.* (2020) demonstrating the intense spectral peak at 1018  $\text{cm}^{-1}$  which was assigned to the C-O stretching of the polysaccharide group in *C. albicans* biofilm. Furthermore, the spectral peaks in the range between 1200  $\text{cm}^{-1}$  and 900  $\text{cm}^{-1}$  have also been assigned to the polysaccharide in other spectroscopic studies of *C. albicans* (Sandt *et al.*, 2003; Adt *et al.*, 2006; Lal *et al.*, 2010; Taha *et al.*, 2013). Moreover, the spectral peaks at 810  $\text{cm}^{-1}$ , 809  $\text{cm}^{-1}$ , 808  $\text{cm}^{-1}$  and 807  $\text{cm}^{-1}$  representing the  $\alpha$ -mannans in *Candida utilis* have also been reported (Křižková *et al.*, 2001; Taha *et al.*, 2013).

The viability of biofilms is one of the important pathogenic characteristics of microorganisms that can cause a broad spectrum of diseases. An insightful elucidation of the viability of microbial biofilms can

direct the strategies for biofilm control. The present study used a resazurin assay to evaluate the viability of *C. albicans* biofilm in the presence of antifungals and the results suggested that the best antibiofilm agent is the econazole nitrate-based antifungal cream as it showed the lowest  $\text{IC}_{50}$  value. The inhibition of *C. albicans* biofilm by the antifungals demonstrated herein is probably mediated by the changes in lipid, protein, nucleic acid, and polysaccharide compositions. According to several works, biochemical changes in the biofilm following antimicrobial treatment are useful to provide an insight into the mode of action of the antibiofilm agent (Suci *et al.* 1994; Yahya *et al.* 2018; Johari *et al.* 2020; Zawawi *et al.* 2020; Villa *et al.* 2021). Meanwhile, Tantala *et al.* (2019) demonstrated that there was a shift of an FTIR spectral peak of *Listeria innocua* cells from 1650  $\text{cm}^{-1}$  (Amide I of  $\alpha$ -helix structure) to 1630  $\text{cm}^{-1}$  (Amide I of  $\beta$ -pleated sheet structures) due to the antibacterial activity of chitosan. They suggested that the changes in the FTIR spectral peaks of the protein components might be due to the denaturation of proteins and alteration of the cell membrane, leading to cell damage and death. The published information related to the effect of imidazole antifungal agents on the FTIR spectra of *Candida* biofilms is still scarce. Thus, these findings may provide the first evidence of FTIR spectral changes of *C. albicans* biofilm following the treatment with econazole nitrate, miconazole nitrate, ketoconazole, and tolnaftate-based antifungal creams.

## CONCLUSION

From the study that had been carried out, econazole nitrate, miconazole nitrate, ketoconazole, and tolnaftate-based antifungal creams had effectively inhibited the viability of *C. albicans* biofilm. The biofilm inhibition was found to be associated with the FTIR spectral changes in the range between 3000  $\text{cm}^{-1}$  and 600  $\text{cm}^{-1}$ . Therefore, these findings may develop an important biochemical insight into how the imidazole antifungals control *C. albicans* biofilm.

## ACKNOWLEDGEMENTS

This research was funded by the Malaysian Ministry of Higher Education under Fundamental Research Grant Scheme, (FRGS/1/2019/STG04/UITM/02/2).

## CONFLICT OF INTEREST

The authors declare no conflict of interest.

## REFERENCES

Abd, E.R.M., Mohamed, D., Abo, M., Ela, E., Fadl, G. & Gad, M. 2014. N-acetylcysteine inhibits and eradicates *Candida albicans* biofilms. *American*

- Journal of Infectious Diseases and Microbiology*, **2(5)**: 122–130. <https://doi.org/10.12691/ajidm-2-5-5>
- Adt, I., Toubas, D., Pinon, J., Mi., Manfait, M. & Sockalingum, G.D. 2006. FTIR spectroscopy as a potential tool to analyse structural modifications during morphogenesis of *Candida albicans*. *Archives of Microbiology*, **185(4)**: 277–285. <https://doi.org/10.1007/s00203-006-0094-8>
- Aging, T. & Munajad, A. 2018. Fourier transform infrared (FTIR) spectroscopy analysis of transformer paper in mineral oil-paper composite insulation under accelerated thermal aging. *Energies*, **11**: 364. <https://doi.org/10.3390/en11020364>
- Alsterholm, M., Karami, N. & Faergemann, J. 2010. Antimicrobial activity of topical skin pharmaceuticals – an in vitro study. *Acta Dermato-Venereologica*, **90**: 239–245. <https://doi.org/10.2340/00015555-0840>
- Berthomieu, C. & Hienerwadel, R. 2009. Fourier transform infrared (FTIR) spectroscopy. *Photosynthesis Research*, **101(2)**: 157–170. <https://doi.org/10.1007/s11120-009-9439-x>
- Bhat, R. 2013. Potential use of Fourier transform infrared spectroscopy for identification of molds capable of producing mycotoxins. *International Journal of Food Properties*, **16(8)**: 1819–1829. <https://doi.org/10.1080/10942912.2011.609629>
- Bojsen, R., Regenber, B. & Folkesson, A. 2014. *Saccharomyces cerevisiae* biofilm tolerance towards systemic antifungals depends on growth phase. *BMC Microbiology*, **14(1)**: 1–10. <https://doi.org/10.1186/s12866-014-0305-4>
- Bombalska, A., Mularczyk-Oliwa, M., Kwaśny, M., Włodarski, M., Kaliszewski, M., Kopczyński, K. & Trafny, E.A. 2011. Classification of the biological material with use of FTIR spectroscopy and statistical analysis. *Spectrochimica Acta - Part A: Molecular and Biomolecular Spectroscopy*, **78(4)**: 1221–1226. <https://doi.org/10.1016/j.saa.2010.10.025>
- Coban, A.Y., Uzun, M., Akgunes, A. & Durupinar, B. 2012. Comparative evaluation of the microplate nitrate reductase assay and the rezasurin microtitre assay for the rapid detection of multidrug resistant *Mycobacterium tuberculosis* clinical isolates. *Memórias Do Instituto Oswaldo Cruz*, **107(5)**: 578–581. <https://doi.org/10.1590/s0074-02762012000500002>
- Essendoubi, M., Toubas, D., Bouzaggou, M., Pinon, J.M., Manfait, M. & Sockalingum, G.D. 2005. Rapid identification of *Candida* species by FT-IR microspectroscopy. *Biochimica et Biophysica Acta - General Subjects*, **1724(3)**: 239–247. <https://doi.org/10.1016/j.bbagen.2005.04.019>
- Fiołka, M.J., Mieszawska, S., Czaplewska, P., Szymańska, A., Stępnik, K., Chmiel, W.S. & Lewtak, K. 2020. *Candida albicans* cell wall as a target of action for the protein – carbohydrate fraction from coelomic fluid of *Dendrobaena veneta*. *Scientific Reports*, **10**: 1–19. <https://doi.org/10.1038/s41598-020-73044-w>
- Gebremedhin, S., Dorocka-Bobkowska, B., Prylinski, M., Konopka, K. & Duzgunes, N. 2014. Miconazole activity against *Candida* biofilms developed on acrylic discs. *Journal of Physiology and Pharmacology*, **65(4)**: 593–600.
- Gulati, M. & Nobile, C.J. 2016. *Candida albicans* biofilms: development, regulation and molecular mechanisms. *Microbes and Infection*, **18(5)**: 310–321. <https://doi.org/10.1016/j.micinf.2016.01.002>
- Hani, U., Shiva, G., Vaghela, R., Osmani, R.A.M. & Shrivastava, A. 2015. Candidiasis : A fungal infection- current challenges and progress in prevention and treatment. *Infectious Disorders – Drug Targets*, **15(1)**: 42–52. <https://doi.org/10.2174/1871526515666150320162036>
- Hasan, F., Xess, I., Wang, X., Jain, N. & Fries, B.C. 2009. Biofilm formation in clinical *Candida* isolates and its association with virulence. *Microbes and Infection*, **11(8–9)**: 753–761. <https://doi.org/10.1016/j.micinf.2009.04.018>
- Isa, S.F.M., Hamid, U.M.A. & Yahya, M.F.Z.R. 2022. Treatment with the combined antimicrobials triggers proteomic changes in *P. aeruginosa*-*C. albicans* polyspecies biofilms. *ScienceAsia*, **48(2)**: 215–222. <https://doi.org/10.2306/scienceasia1513-1874.2022.020>
- Johari, N.A., Amran, S.S.D., Kamaruzzaman, A.N.A., Man, C.A.I.C. & Yahya, M.F.Z.R. 2020. Antibiofilm potential and mode of action of Malaysian plant species: A review. *Science Letters*, **14**: 34–46. <https://doi.org/10.24191/sl.v14i2.9541>
- Křižková, L., Ďuračková, Z., Šandula, J., Sasinková, V. & Krajčovič, J. 2001. Antioxidative and antimutagenic activity of yeast cell wall mannans in vitro. *Mutation Research - Genetic Toxicology and Environmental Mutagenesis*, **497(1–2)**: 213–222. [https://doi.org/10.1016/S1383-5718\(01\)00257-1](https://doi.org/10.1016/S1383-5718(01)00257-1)
- Lal, P., Sharma, D., Pruthi, P. & Pruthi, V. 2010. Exopolysaccharide analysis of biofilm-forming *Candida albicans*. *Journal of Applied Microbiology*, **109(1)**: 128–136. <https://doi.org/10.1111/j.1365-2672.2009.04634.x>
- Marak, M.B. & Dhanashree, B. 2018. Antifungal susceptibility and biofilm production of *Candida* spp. isolated from clinical samples. *International Journal of Microbiology*, **2018**: 7495218. <https://doi.org/10.1155/2018/7495218>
- Naseer, K., Ali, S. & Qazi, J. 2020. ATR-FTIR spectroscopy as the future of diagnostics: a systematic review of the approach using biofluids. *Applied Spectroscopy Reviews*, **56**: 85–97. <https://doi.org/10.1080/05704928.2020.1738453>

- Natalello, A., Ami, D., Brocca, S., Lotti, M. & Doglia, S.M. 2005. Secondary structure, conformational stability and glycosylation of a recombinant *Candida rugosa* lipase studied by Fourier-transform infrared spectroscopy. *Biochemical Journal*, **385**(2): 511–517. <https://doi.org/10.1042/BJ20041296>
- Othman, N.A. & Yahya, M.F.Z.R. 2019. In silico analysis of essential gene and non-homologous proteins in *Salmonella typhimurium* biofilm. *Journal of Physics: Conference Series*, **1349**: 012133. <https://doi.org/10.1088/1742-6596/1349/1/012133>
- Pebotuwa, S., Kochan, K., Peleg, A., Wood, B.R. & Heraud, P. 2020. Influence of the sample preparation method in discriminating *Candida* spp. using ATR-FTIR spectroscopy. *Molecules*, **25**(7): 1551. <https://doi.org/10.3390/molecules25071551>
- Qiu, W., Ren, B., Dai, H., Zhang, L., Zhang, Q., Zhou, X. & Li, Y. 2017. Clotrimazole and econazole inhibit *Streptococcus mutans* biofilm and virulence in vitro. *Archives of Oral Biology*, **73**: 113–120. <https://doi.org/10.1016/j.archoralbio.2016.10.011>
- Quilès, F., Accoceberry, I., Couzigou, C., Francius, G., Noël, T. & El-Kirat-Chatel, S. 2017. AFM combined to ATR-FTIR reveals *Candida* cell wall changes under caspofungin treatment. *Nanoscale*, **9**(36): 13731–13738. <https://doi.org/10.1111/j.1567-1364.2006.00117.x>
- Ramage, G., Martinez, J.P. & Lopez-ribot, J.L. 2006. *Candida* biofilm on implanted biomaterials: a clinically significant problem. *FEMS Yeast Research*, **6**(7): 979–986.
- Ryder, N.S., Frank, I. & Dupont, M. 1986. Ergosterol biosynthesis inhibition by the thiocarbamate antifungal agents tolnaftate and tolclolate. *Antimicrobial Agents and Chemotherapy*, **29**(5): 858–860. <https://doi.org/10.1128/AAC.29.5.858>
- Sandt, C., Sockalingum, G.D., Aubert, D., Lapan, H., Lepouse, C., Jaussaud, M. & Toubas, D. 2003. Use of fourier-transform infrared spectroscopy for typing of *Candida albicans* strains isolated in intensive care units. *Journal of Clinical Microbiology*, **41**(3): 954–959. <https://doi.org/10.1128/JCM.41.3.954-959.2003>
- Shapaval, V., Brandenburg, J., Blomqvist, J., Tafintseva, V. & Passoth, V. 2019. Biotechnology for biofuels biochemical profiling, prediction of total lipid content and fatty acid profile in oleaginous yeasts by FTIR spectroscopy. *Biotechnology for Biofuels*, **12**(1): 1–12. <https://doi.org/10.1186/s13068-019-1481-0>
- Shi, Q., Câmara, C.R.S. & Schlegel, V. 2018. Biochemical alterations of *Candida albicans* during the phenotypic transition from yeast to hyphae captured by Fourier transform mid-infrared- attenuated reflectance spectroscopy. *The Analyst*, **143**: 5404–5416. <https://doi.org/10.1039/c8an01452c>
- Silva, S., Rodrigues, C.F., Ara, D., Rodrigues, M.E. & Henriques, M. 2017. *Candida* species biofilms' antifungal resistance. *Journal of Fungi*, **3**(1): 8. <https://doi.org/10.3390/jof3010008>
- Suci, P.A., Mittelman, M.W., Yu, F.P. & Geesey G.G. 1994. Investigation of ciprofloxacin penetration into *Pseudomonas aeruginosa* biofilms. *Antimicrob Agents Chemother*, **38**: 2125–2133. <https://doi.org/10.1128/AAC.38.9.2125>
- Sockalingum, G.D., Sandt, C., Toubas, D., Gomez, J., Pina, P., Beguinot, I. & Manfait, M. 2002. FTIR characterization of *Candida* species: A study on some reference strains and pathogenic *C. albicans* isolates from HIV+patients. *Vibrational Spectroscopy*, **28**(1): 137–146. [https://doi.org/10.1016/S0924-2031\(01\)00152-7](https://doi.org/10.1016/S0924-2031(01)00152-7)
- Taha, M., Hassan, M., Essa, S. & Tartor, Y. 2013. Use of Fourier transform infrared spectroscopy (FTIR) spectroscopy for rapid and accurate identification of yeasts isolated from human and animals. *International Journal of Veterinary Science and Medicine*, **1**(1): 15–20. <https://doi.org/10.1016/j.ijvsm.2013.03.001>
- Vandenbosch, D., Braeckmans, K., Nelis, H.J. & Coenye, T. 2010. Fungicidal activity of miconazole against *Candida* spp. biofilms. *Journal of Antimicrobial Chemotherapy*, **65**(4): 694–700. <https://doi.org/10.1093/jac/dkq019>
- Villa, F., Secundo, F., Forlani, F. *et al.* 2010. Biochemical and molecular changes of the zosteric acid-treated *Escherichia coli* biofilm on a mineral surface. *Annals of Microbiology*, **71**(3). <https://doi.org/10.1186/s13213-020-01617-1>
- Waghule, T., Sankar, S., Rapalli, V.K., Gorantla, S., Dubey, S.K., Chellappan, D.K. & Singhvi, G. 2020. Emerging role of nanocarriers based topical delivery of anti-fungal agents in combating growing fungal infections. *Dermatologic Therapy*, **33**(6): 1–34. <https://doi.org/10.1111/dth.13905>
- Yaacob M.F., Murata, A., Nor, N.H.M., Jesse, F.F.A & Yahya, M.F.Z.R. 2021. Biochemical composition, morphology and antimicrobial susceptibility pattern of *Corynebacterium pseudotuberculosis* biofilm. *Journal of King Saudi University – Science*, **33**: 101225. <https://doi.org/10.1016/j.jksus.2020.10.022>
- Yahya, M.F.Z.R., Hamid, U.M.A., Norfatimah, M.Y. & Kambol, R. 2014. In silico analysis of essential tricarboxylic acid cycle enzymes from biofilm-forming bacteria. *Trends in Bioinformatics*, **7**: 26. <https://doi.org/10.3923/tb.2014.19.26>
- Yahya, M.F.Z., Alias, Z. & Karsani, S.A. 2018. Antibiofilm activity and mode of action of DMSO alone and its combination with afatinib against Gram-negative pathogens. *Folia Microbiologica*,

- 63: 23–30. <https://doi.org/10.1007/s12223-017-0532-9>
- Zawawi, W.M.A.W.M., Ibrahim, M.S.A., Rahmad, N., Hamid, U.M.A. & Yahya, M.F.Z.R. 2020. Proteomic analysis of *Pseudomonas aeruginosa* treated with *Chromolaena odorata* extracts. *Malaysian Journal of Microbiology*, **16(2)**: 124-133. <https://doi.org/10.21161/mjm.190512>
- Zhang, Li, B., Wang, Q., Wei, X., Feng, W., Chen, Y. & Huang, P. 2017. Application of Fourier transform infrared spectroscopy with chemometrics on postmortem interval estimation based on pericardial fluids. *Scientific Reports*, **7(1)**: 1–8. <https://doi.org/10.1038/s41598-017-18228-7>